Etching or Stabilization of GaAs(001) under Alkali and Halogen Adsorption

ARTICLE *in* THE JOURNAL OF PHYSICAL CHEMISTRY C · APRIL 2012

Impact Factor: 4.77 · DOI: 10.1021/jp211360d

THE JOURNAL OF PHYSICAL CHEMISTRY C

Article

pubs.acs.org/JPCC

Etching or Stabilization of GaAs(001) under Alkali and Halogen Adsorption

O. E. Tereshchenko,[*,†,‡] D. Paget,[§] K. V. Toropetsky,[†] V. L. Alperovich,[†,‡] S. V. Eremeev,[∥,⊥] A. V. Bakulin,[∥,⊥] S. E. Kulkova,[∥,⊥] B. P. Doyle,[#,▽] and S. Nannarone[#,○]

[†]Institute of Semiconductor Physics, Novosibirsk, 630090 Russian Federation

[‡]Novosibirsk State University, Novosibirsk, 636090 Russian Federation

[§]Physique de la matière condensée, Ecole Polytechnique, CNRS, F-91128 Palaiseau, France

[∥]Institute of Strength Physics and Materials Science, Tomsk, 636021 Russian Federation

[⊥]Tomsk State University, Tomsk, 634050 Russian Federation

[#]Laboratorio Nazionale TASC, INFM-CNR, 34012 Trieste, Italy

[▽]University of Johannesburg, Auckland Park 2006, South Africa

[○]Dipartimento di Ingegneria dei Materiali e dell'Ambiente, Universita di Modena e Reggio Emilia and CNISM, Via Vignolese 905, 41100 Modena, Italy

ABSTRACT: Experimentally and by ab initio calculations it is shown that adsorption of electropositive cesium on the As-rich surface of GaAs(001) and, in a symmetric fashion, adsorption of electronegative iodine on the Ga-rich surface, induce a decrease of the surface stability, thus facilitating surface etching. Conversely, Cs adsorption on the Ga-rich surface and I adsorption on the As-rich surface lead to an increased surface stability. Etching occurs when adsorption-induced charge transfer weakens the backbonds of the top arsenic atoms for the case of Cs on the As-rich $\beta2(2 \times 4)$ surface and the lateral bonds in the topmost surface layer for I on the Ga-rich $\zeta(4 \times 2)$ surface. The possibilities of reversible transitions between the two reconstructed surfaces and of atomic layer etching with monolayer precision are demonstrated.

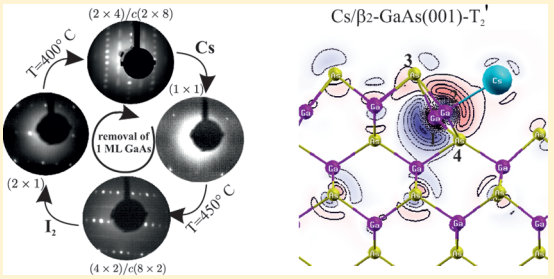

INTRODUCTION

The advanced modifications of epitaxial growth techniques such as migration enhanced and atomic layer epitaxies[1,2] allow one to grow semiconductor structures in which the interface smoothness and the thickness of layers are controlled with the ultimate precision of one monolayer. Along with atomic-layer growth, for modern nanotechnology, it is important to develop techniques of atomic-layer ("digital") etching, which consist of layer-by-layer removal of a semiconductor with monolayer resolution. For III−V semiconductors, atomic layer etching can be realized by using adsorbates, which selectively react with polar surfaces enriched with elements of III or V groups and thus allow selective removal of surface cations or anions. It was shown in ref 3 that iodine adsorption on the Ga-rich GaAs(001) surface, followed by low-temperature annealing, led to the desorption of gallium iodides GaI_x and conversion to the As-rich surface with a (2×4) reconstruction. Conversely, the adsorption of cesium on the As-rich GaAs(001)-(2×4) surface facilitates low-temperature removal of surface arsenic and back transfer to the Ga-rich (4×2) reconstruction.[4] Although alternate depositions of iodine and cesium followed by low-temperature anneals[5] can be used for in situ atomic layer etching of GaAs(001), the mechanisms underlying this opportunity are not clear. Because charge exchange from the electropositive Ga to electronegative As is known to stabilize the polar GaAs(001) surface,[6] it can be anticipated that adsorption of electronegative (halogen) or electropositive (alkaline) elements on anion-rich and cation-rich GaAs(001), respectively, leads to an opposite transfer and therefore to a weakening of the backbonds of the topmost atoms. However, this is an essentially electronic mechanism that could be neither proved nor rejected by the structural data presented in refs 4 and 5 as well as by other previous results on the I/GaAs(001) and Cs/GaAs(001) surfaces.[3,7−11]

The present work is aimed at the elucidation of the microscopic mechanisms of the selective interaction of iodine and cesium with As-rich $\beta2(2 \times 4)$ and Ga-rich $\zeta(4 \times 2)$ reconstructed GaAs(001) surfaces by means of photoemission spectroscopy and ab initio calculations, which yield information on the electronic properties of the surfaces. It is found that the "weakening of backbonds" mechanism is not universal and is responsible for the decrease in surface stability only for the Cs/

Received: November 25, 2011
Revised: March 23, 2012
Published: March 29, 2012

   dx.doi.org/10.1021/jp211360d | J. Phys. Chem. C 2012, 116, 8535−8540

$\beta 2$ surface. In contrast, for the I/ζ surface a different mechanism occurs, which involves the weakening of the lateral bonds in the topmost surface layer.

EXPERIMENTAL SECTION

Clean reconstructed surfaces of epitaxial p-type GaAs(001) were obtained by removing oxides in HCl in isopropyl alcohol (HCl-iPA) under a dry nitrogen atmosphere, transfer to ultrahigh vacuum (UHV) setups without exposure to air, and subsequent annealing in vacuum.[12] The surface structure was studied by low-energy electron diffraction (LEED).[4,5,12] Photoemission experiments were performed at the BEAR beamline of the ELETTRA storage ring (Trieste, Italy) in a UHV chamber with a base pressure in the low 10^{-10} mbar range, equipped with a hemispherical analyzer. The angle between the photon beam and the normal to the sample surface was 45°. Exposures to iodine and cesium were performed at room temperature (RT). Iodine was deposited using a solid electrochemical cell containing Ag_4RbI_5.[5,13] Cesium was deposited from thoroughly outgassed dispensers. Calibrations of the Cs and I coverages were performed by monitoring the integrated intensities of the Cs 4d and I 4d core level spectra (CLS), respectively. Under exposure, both of these intensities saturate at a coverage taken to be 1 ML.[3,14]

RESULTS AND DISCUSSION

The selective atomic layer etching is first illustrated in Figure 1. Panel a shows the LEED pattern of the starting As-rich surface

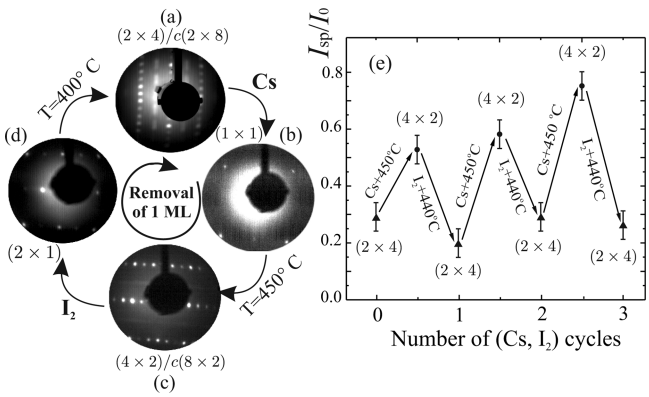

Figure 1. Evolution of the LEED patterns (a–d) under multiple Cs–I adsorption and desorption cycles. (a) Clean As-rich (2 × 4)/c(2 × 8) surface, (b) after successive adsorption of 0.5 ML of Cs, (c) annealing to 450 °C, and (d) adsorption of 0.5 ML of iodine. Successive annealing to 400 °C of I-covered surface (d) recovered the initial As-rich surface with (2 × 4)/c(2 × 8) reconstruction (a). The right panel (e) shows the ratio of the diffraction spots' intensity I_{sp} to the total intensity I_0 of the LEED image versus the number of the cesium and iodine adsorption–desorption cycle. The iodine coverage on the surface was 0.3, 0.5, and 1 ML in the first, second, and third cycles, respectively.

with a (2 × 4) reconstruction obtained by removing oxides in HCl-iPA and annealing in vacuum at 450 °C. Adsorption of 0.5 ML of Cs leads to a diffuse (1 × 1) LEED pattern (Figure 1b). Subsequent annealing to 450 °C gives a sharp (4 × 2)/c(8 × 2) reconstruction, which is characteristic of the Ga-rich surface (Figure 1c). The decrease in surface stability is revealed by the lowering by ~100 °C of the annealing temperature necessary to obtain the (4 × 2)/c(8 × 2) reconstruction. After subsequent adsorption of 0.5 ML of iodine, the surface exhibits a diffuse (2 × 1) LEED pattern (Figure 1d). The starting surface with a (2 × 4)/c(2 × 8) reconstruction is finally recovered after annealing to 400 °C. We infer that the whole cycle has removed one monolayer of GaAs. The above results show that adsorption of Cs on the (2 × 4)/c(2 × 8) surface and of I_2 on the (4 × 2)/c(8 × 2) surface leads to a decrease in the surface stability. In the converse case of Cs adsorption on the (4 × 2)/c(8 × 2) surface[4] and of iodine on the (2 × 4)/c(2 × 8) surface,[11] it is known that the surface stability is increased so that under annealing the adsorbed layer is desorbed and the underlying surface reconstruction is recovered. As seen from Figure 1e, each Cs–I_2 cycle also leads to an increase in the intensity of the LEED spots for the (4 × 2)/c(8 × 2) surface, which shows that the surface quality has improved.[5]

Shown in Figure 2 are the Ga 3d and As 3d CLS of the clean surfaces, of the same surfaces after adsorption, and their differences. The detailed decomposition of the measured spectra into bulk and surface components (not shown here) proves the rise of adsorbate-induced components in the CLS. These CLS changes are clearly demonstrated in the differential spectra shown in Figure 2. For adsorption on a cation (anion)-rich surface in the stabilization regime (the left (a,e) and right (d,h) columns), the most significant change concerns the CLS of this cation (anion) atom, whereas a smaller change of the CLS is observed for the other atom. Indeed, adsorption of Cs on the Ga-rich surface induces a small but clearly detected modification of the Ga 3d CLS (Figure 2e). Decomposition proves that the intensity of the chemically shifted component decreases by ~20%. The As 3d CLS remains practically unchanged (Figure 2a). In the same way, for I_2 adsorption on the As-rich surface, the situation is the opposite: the Ga 3d CLS modification is very weak (Figure 2h), whereas the As 3d CLS changes significantly (Figure 2d). One can conclude that in the stabilizing regime the adsorbate-induced charge redistribution causes neither charge redistribution between surface substrate atoms nor changes in the bond energies.

In contrast, in the etching regime (the two middle columns in Figure 2b,c,f,g), the differences between spectra show significant changes of *both* the cation and anion CLS. In particular, for As 3d under Cs deposition on the GaAs(001)-(2 × 4) surface (Figure 2b), a negative signal is observed at a positive binding energy, together with a positive signal at a negative binding energy. For Ga 3d (Figure 2f), only the negative signal at a positive binding energy is observed because as shown independently[15] the corresponding positive signal is degenerate with the bulk contribution and is not apparent. Similarly, strong changes of CLS are observed at the I/GaAs(001)-(4 × 2) surface (Figure 2c,g). A qualitative conclusion is then derived, according to which the etching behavior induces a modification not only of the configuration of topmost atoms but also of atoms of the second atomic layer, thereby altering the stability of the surface.

CLS yield the effective charge sitting on surface atoms and thus render information on the ionic part of the binding energy and its change under adsorption. The adatom-induced changes in the covalent part of the binding energy, which are determined by the charge density redistribution between the atoms, have a weaker influence on the photoemission spectra. To obtain a microscopic explanation of the photoemission results and to verify the hypothesis of the weakening of the backbonds as a reason for the adatom-induced etching behavior, we performed density functional theory calculations

dx.doi.org/10.1021/jp211360d | J. Phys. Chem. C 2012, 116, 8535–8540

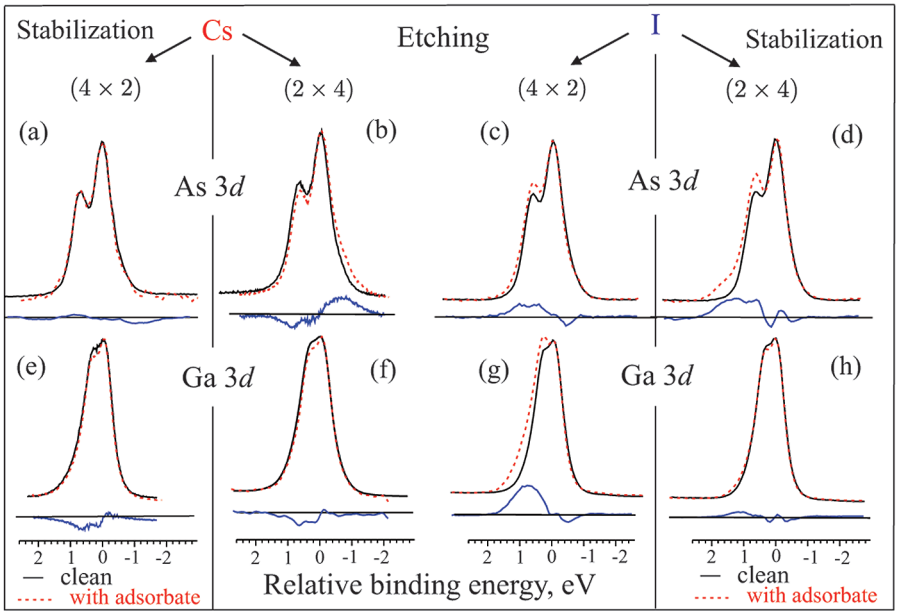

Figure 2. Ga 3d and As 3d core level spectra (CLS) for 0.3 ML adsorption of Cs and I on the (2 × 4) and (4 × 2) surfaces. Shown in solid lines are CLS of the clean surfaces, while the spectra after adsorption are shown in dotted lines, for cases where adsorption increases the surface stability or facilitates surface etching. Also shown are differences showing the adsorbate-induced modification of the CLS.

of the surface atomic and electronic structure using the VASP code.[16,17] The interaction between the ion cores and valence electrons was described by the projector augmented-wave method.[18,19] The generalized gradient approximation (GGA)[20] was used to describe the exchange correlation energy. Details are given in ref 21.

As shown by the ball-and-stick model (Figure 3a,c), the $\beta 2$ unit cell of the (2 × 4) reconstruction of the As-rich surface exhibits two As dimers at the top surface and a third As dimer in the third atomic layer. The top atomic layer of the ζ unit cell

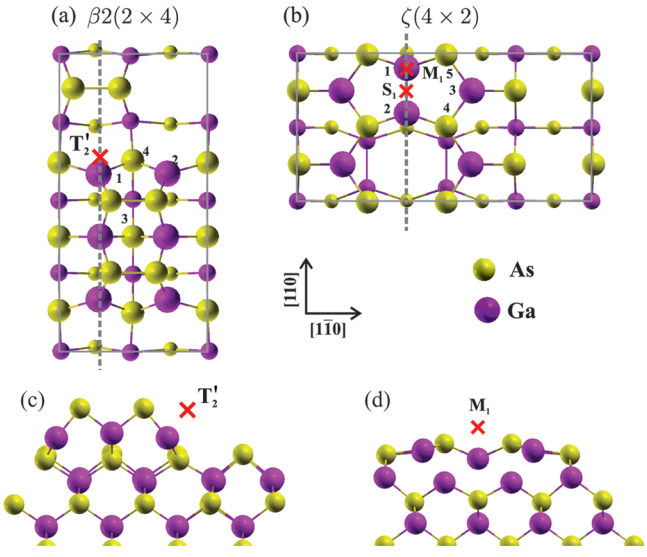

Figure 3. Plane views (a,b) and side views (c,d) of ball-and-stick models of the As-rich $\beta 2(2 \times 4)$ (a,c) and of the Ga-rich $\zeta(4 \times 2)$ (b,d) surface unit cells of GaAs(001). Ga atoms are shown in purple while As atoms are shown in yellow. Projections of preferable adsorption sites on the surface are depicted by red crosses. Gray dashed lines show the positions of section planes given in Figures 4 and 5.

of the (4 × 2) reconstruction, shown in Figure 3b,d, contains six Ga and eight As atoms. There is one Ga dimer that is located lower than the nearest As atoms, whereas the underlying layer contains two Ga dimers.

The results of the calculations allowed us to determine the positions of atoms on the clean and adsorbate-covered surfaces, the spatial distribution of the electron density, and the magnitudes of the charge transfer and the binding energies of surface atoms. Changes in the binding energy of the surface atoms closest to the adsorbed atom were calculated as the difference of the total energies of the system after the removal of the surface dimerized atoms from the $\beta 2(2 \times 4)$ with adsorbed cesium (iodine) and the clean surface: $\Delta E = (E_{ad/GaAs} - E_{ad/GaAs-As_{dim}}) - (E_{GaAs} - E_{GaAs-As_{dim}})$, where $E_{ad/GaAs}(E_{GaAs})$ and $E_{ad/GaAs-As_{dim}}(E_{GaAs-As_{dim}})$ are the total energies of the system before and after removal of the surface atoms with (without) the adsorbed atom. The adsorbate-induced modifications of the electronic charge at position r were defined by $\Delta\rho(r) = \rho_{GaAs}(r) + \rho_{Cs(I)}(r) - \rho_{Cs(I)/GaAs}(r)$. It is found that for the two surfaces the preferential adsorption sites of both Cs and I are all near Ga atoms, which belong to the top layer for the Ga-rich reconstruction and to the second layer for the As-rich one. It should be noted that the presence of adsorption sites with similar binding energies is a general problem for the comparison of experimental results with calculations for reconstructed semiconductor surfaces. In this study, we selected the adsorption sites that are both energetically favorable and produce prominent charge redistribution effects at the surface. For the $\beta 2(2 \times 4)$ surface, the most favorable site is the T_2' site near the empty dangling bond of the Ga atom labeled 1 in Figure 3a, bonded to the first layer As atoms by backbonds.[7] The selection of a single adsorption site T_2' for the As-rich surface may seem to be inconsistent with the diffuse (1 × 1) LEED pattern, which presumably means a random distribution of adsorption sites before annealing. It should be noted, however, that according to a previous LEED study,[4] at small coverages 0.1 to 0.3 ML the deposition of Cs preserves the

dx.doi.org/10.1021/jp211360d | J. Phys. Chem. C 2012, 116, 8535−8540

surface reconstructions of both the Ga-rich $\zeta(4 \times 2)$ and As-rich $\beta2(2 \times 4)$ surfaces. This fact conforms with the assumption that on each surface the dominant occupation of a single type of sites takes place. On the Ga-rich surface, further cesium deposition leads to ordered adsorption up to 0.7 ML, whereas it causes a fast disorder of the As-rich $\beta2(2 \times 4)$ surface reconstruction at Cs coverages above 0.3 ML.[4] (See the diffuse (1×1) LEED image in Figure 1b.) However, for coverages corresponding to more than one adatom per particular adsorption site in a surface unit cell, these calculations are not applicable anyway because the occupation of other sites is inevitably involved. The case of multisite occupation at large coverages is readily accessible in the experiment but is far more complicated for the theoretical analysis, as compared with the single-site case. Therefore, here we can speculate only that the trends revealed by the DFT calculations for small Cs coverages are preserved for larger coverages.

Figure 4 gives the map of the section of $\Delta\rho(r)$ for the As-rich surface with adsorbed Cs and I. This section, which is shown in Figure 3a, is perpendicular to the surface, passes through the adsorbate, and includes also the dangling bond of the second layer Ga atom. The middle panel shows the dependence as a function of depth z of the integral of $\Delta\rho(r)$ over the planes parallel to the surface. It is seen that on the As-rich $\beta2(2 \times 4)$ surface the T_2' cesium induces a dipole located at the second-layer Ga atoms with a charge transfer of 0.6 e from Cs to the GaAs surface, in agreement with ref 7. This explains the chemical shift toward lower binding energies observed in the Ga 3d CLS. (See Figure 2f). A small amount of charge is transferred to the antibonding orbitals of As dimers, which explains the modification of the As 3d CLS. The charge profile $\Delta\rho(z)$ reveals a cesium-induced reduction of the electron density for z from 0 to −2 Å, that is, between the surface arsenic atoms and lower lying gallium atoms. This is equivalent to the appearance of "holes" on the As−Ga backbonds and leads to their weakening. It is interesting to note that under Cs adsorption the As−Ga bond keeps almost the same bond length, although the Ga atom moves inward by 1 Å in the direction perpendicular to the bond (Figure 4a). This probably means that here the decrease in the binding energy of the As atom is the consequence of atomic shifts and charge redistribution in a complex multiatomic system (the computational cell consists of 82 atoms); therefore, it has no direct correlation with the specific bond length, unlike a diatomic molecule. At this moment, we cannot elucidate a single reason for keeping the bond length nearly constant. Possible reasons may consist of a steric hindrance or influence of strain. The latter possibility is indirectly supported by the estimation of the energy increase of 0.38 eV per cell induced by Ga atom shift without Cs atom.

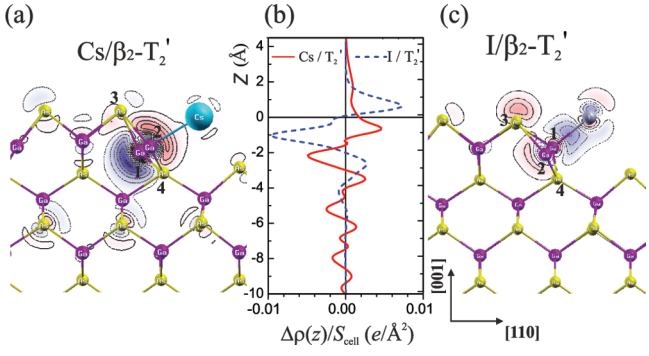

Figure 4. Maps show the charge density difference $\Delta\rho(r)$ for adsorption of Cs and I at the T_2' site of the As-rich surface through the section shown in Figure 3a. Shown in red (blue) are regions of charge excess (depletion). Also shown for clarity are projections of the atomic positions on the same plane. The center panel shows the $\Delta\rho$ integrated over the xy plane. The zero of distance is taken at the position of the adsorbed atom. S_{cell} is the area of the surface cell.

The calculated Cs-induced decrease in the binding energy of surface As atoms is equal to 0.14 eV per bond, which yields the decrease in the As dimer binding energy E_d by ΔE_d = 0.56 eV. Using the exponential dependence for the dimer desorption rate $\Gamma = \Gamma_0 \exp(-E_d/k_BT)$, where Γ_0 is a prefactor, T is the surface temperature, and k_B is the Boltzmann constant, the value of E_d = 5.5 eV obtained in ref 22 and the experimental Cs-induced decrease in desorption temperature from 550 °C for clean As-rich surface to 450 °C for the surface with Cs, we obtained an experimental estimation of $\Delta E_d \approx 0.67$ eV, which is in reasonable agreement with the calculated value.

For I adsorption on the T_2' site of the same As-rich surface, the situation is opposite to that found for Cs and corresponds to surface stabilization because the charge difference shows electron depletion above the top As, and to some extent below the Ga(2) atom, and electron accumulation in the I−Ga chemical bond. Therefore, in agreement with the photoemission results of Figure 2d,h, most of the electron density from the top As accumulates in the I−Ga bond, which keeps the charge environment of second-layer Ga atoms almost unchanged. The estimated binding energy change of the surface dimer arsenic atoms is small $|\Delta E_d(I/\beta2)| \leq 0.03$ eV.

Shown in Figure 5 are the results for adsorption at the Ga-rich surface, with charge distribution maps taken in the plane containing both the adsorbate and Ga dimer (Figure 3b). For the $\zeta(4 \times 2)$ reconstruction, the most favorable sites are the S_1 Ga dimer bridge site for Cs and the M_1 dimer top site for I. For Cs adsorption at the S_1 site the formed dipole is due to the polarization of subsurface atoms up to the third atomic layer, that is, substantially deeper than for the $\beta2$ surface (Figure 5b). The photoemission results can also be understood in the following way: the slight change of the Ga 3d CLS is due to the negative charge at dimer atom positions (Ga atoms labeled 1

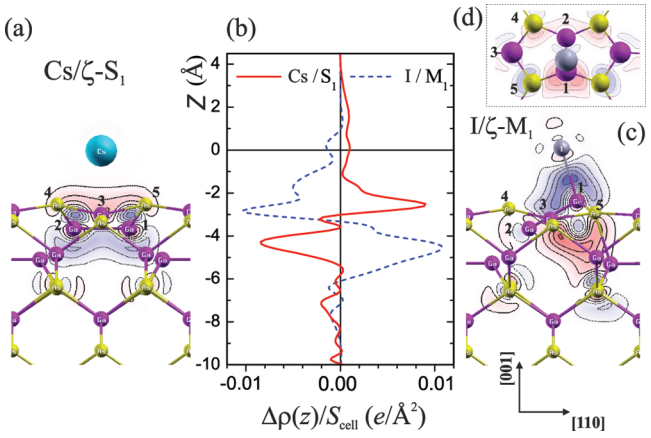

Figure 5. Same as Figure 4 for adsorption of Cs at the S_1 site and of I at the M_1 site of the Ga-rich surface. (For iodine in the M_1 position, a top view is shown in the dashed-line framed inset.)

dx.doi.org/10.1021/jp211360d | J. Phys. Chem. C 2012, 116, 8535−8540

and 2 in Figure 3b), whereas other atoms are relatively far from the S_1 site and have an essentially unperturbed potential. The Ga−As binding energy is found to increase by 0.16 eV, in agreement with the experimental fact that annealing the Cs-covered Ga-rich surface restores the (4×2) structure of the clean surface after Cs desorption.[5]

Shown in Figure 5c,d are the side and top views of the calculated atomic positions and charge distribution maps for the case of iodine adsorption on the $\zeta(4 \times 2)$ surface, which induces the weakening of the surface Ga atom bonds with the substrate and subsequent transfer to the As-rich (2×4) surface under annealing at moderate temperature. The results of the calculations prove that although this effect is similar to the opposite back transfer from the $\beta2(2 \times 4)$ to $\zeta(4 \times 2)$ reconstruction caused by Cs-induced weakening of the surface As atom bonds, the mechanisms of the decrease in the binding energies are qualitatively different for the two cases, mainly due to the differences in the atomic structure and orientations of bonds at the initially clean surfaces. At the $\beta2(2 \times 4)$ surface, the bonds of the top arsenic atoms with lower lying Ga atoms are directed inside the crystal, so the decrease in the binding energy of a top arsenic atom can be interpreted as weakening of its back-bond. It was already mentioned, that under Cs adsorption the length of the As−Ga back-bond remains practically unchanged, and the back-bond weakening is presumably due to the appearance of an effective "hole" on the bond, which is revealed by a decrease in the interlayer electron density between the top As and lower lying Ga atomic layers. In contrast, in the top atomic layer of the clean $\zeta(4 \times 2)$ surface reconstruction the As and Ga atoms lie almost in the same plane due to predominant sp2 hybridization; the dimerized Ga atoms lye even lower than the neighboring As atoms with which they are bind. (See Figure 3b,d). Therefore, the iodine-induced decrease in Ga atom binding energy is discussed in terms of lateral bond rather than back-bond weakening. It is seen from Figure 5c that under adsorption at M1 position, the iodine atom forms a strong bond with one of the dimerized Ga atoms, as visualized in the Figure by the accumulation of electron charge between the I and Ga(1) atoms. As a consequence, the Ga1 atom, which initially lies below the neighboring As atoms (by 1.02 Å), is pulled up by 1.39 Å and lies above the top As atoms. Figure 5d also shows the decrease in electron density between the Ga(1) and neighboring As(5) atoms, that is, the formation of "holes" in the Ga−As bonds. Probably, both the increase in the bond length between Ga(1) and Ga(2) atoms by 0.08 Å and the decrease in electron density between Ga(1) atom and neighboring As atoms contribute to the iodine-induced decrease in the surface Ga(1) atom binding energy and, as a consequence, to the desorption of iodine and gallium under annealing at relatively low temperatures. The calculated decrease in the binding energy averaged over the Ga−Ga and two Ga−As bonds is of 0.86 eV. It is seen from the map of charge distribution shown in Figure 5c that the accumulation of electron charge on the I−Ga(1) bond is compensated by the positive charge, which is strongly delocalized, as compared with the iodine adsorption on the $\beta2(2 \times 4)$ surface (Figure 4c). Therefore, the interpretation of the iodine-induced decrease in the binding energy of Ga atoms in terms of local bond modification should be used with caution.

In summary, it is shown experimentally and theoretically that cesium adsorption on the As-rich GaAs(001) and iodine adsorption on the Ga-rich GaAs(001) reconstructed surfaces lead to a decrease in the binding energy of the surface As and Ga atoms, respectively. Subsequent anneals of the adsorbate-covered surfaces lead to reversible transitions between the surface reconstructions. The results of the ab initio calculations enabled us to elucidate the microscopic mechanisms of the binding energy decrease, which turned out to be different for the Cs/GaAs(001)-$\beta2$ and I/GaAs(001)-ζ surfaces. It should be noted that other halogens and alkali atoms with smaller atomic numbers and covalent radii have stronger, as compared with iodine and cesium, chemical activity under interaction with III−V semiconductor surfaces and thus lead to more rude effects such as the stationary etching of semiconductors by chlorine. On the contrary, the more subtle selective action of I and Cs depends on the composition and structure of the initial clean surface, saturates with increasing adsorbate dose, and is restricted to topmost surface atomic layers. As shown in the present work for the case of GaAs(001), this subtle selectivity yields opportunities for reversible transitions between the surface reconstructions and for atomic layer etching with monolayer precision.

AUTHOR INFORMATION

Corresponding Author

*E-mail: teresh@isp.nsc.ru.

Notes

The authors declare no competing financial interest.

ACKNOWLEDGMENTS

The present work was partially supported by the Russian Foundation for Basic Research. Calculations were performed on the SKIF-Cyberia computer cluster (Tomsk State University).

REFERENCES

(1) Arthur, J. R. *Surf. Sci.* **2002**, *500*, 189.
(2) Ritala, M.; Leskelä, M. *Nanotechnology* **1999**, *10*, 19.
(3) Varekamp, P. R.; Håkansson, M. C.; Kanski, J.; Shuh, D. K.; Björkqvist, M.; Göthelid, M.; Simpson, W. C.; Karlsson, U. O.; Yarmoff, J. A. *Phys. Rev. B* **1996**, *54*, 2101.
(4) Tereshchenko, O. E.; Alperovich, V. L.; Zhuravlev, A. G.; Terekhov, A. S.; Paget, D. *Phys. Rev. B* **2005**, *71*, 155315.
(5) Tereshchenko, O. E.; Toropetsky, K. V.; Alperovich, V. L. *JETP Lett.* **2008**, *87*, 35.
(6) Pashley, M. D. *Phys. Rev. B* **1989**, *40*, 10481.
(7) Hogan, C.; Paget, D.; Garreau, Y.; Sauvage, M.; Onida, G.; Reining, L.; Chiaradia, P.; Corradini, V. *Phys. Rev. B* **2003**, *68*, 205313.
(8) Varekamp, P. R.; Håkansson, M. C.; Kanski, J.; Björkqvist, M.; Göthelid, M.; Kowalski, B. J.; He, Z. Q.; Shuh, D. K.; Yarmoff, J. A.; Karlsson, U. O. *Phys. Rev. B* **1996**, *54*, 2114.
(9) Vedeneev, A. A.; Elstsov, K. N. *JETP Lett.* **2005**, *82*, 44.
(10) Wang, W. K.; Simpson, W. C.; Yarmoff, J. A. *Phys. Rev. B* **2000**, *61*, 2164.
(11) Wang, W. K.; Simpson, W. C.; Yarmoff, J. A. *Phys. Rev. Lett.* **1998**, *81*, 1465.
(12) Tereshchenko, O. E.; Chikichev, S. I.; Terekhov, A. S. *J. Vac. Sci. Technol., A* **1999**, *17*, 2655.
(13) Spencer, N. D.; Goddard, P. J.; Davies, P. W.; Kitson, M.; Lambert, R. M. *J. Vac. Sci. Technol., A* **1983**, *1*, 1554.
(14) Tereshchenko, O. E.; Alperovich, V. L.; Terekhov, A. S. *JETP Lett.* **2004**, *79*, 131.
(15) Tereshchenko, O. E.; Paget, D.; Chiaradia, P.; Wiame, F.; Taleb-Ibrahimi, A. *Phys. Rev. B* **2010**, *81*, 035304.
(16) Kresse, G.; Hafner, J. *Phys. Rev. B* **1993**, *48*, 13115.
(17) Kresse, G.; Furthmüller, J. *Comput. Mater. Sci.* **1996**, *6*, 15.
(18) Blöchl, P. E. *Phys. Rev. B* **1994**, *50*, 17953.

(19) Kresse, G.; Joubert, D. *Phys. Rev. B* **1999**, *59*, 1758.
(20) Perdew, J. P.; Burke, K.; Ernzerhof, M. *Phys. Rev. Lett.* **1996**, *77*, 3865.
(21) Kulkova, S. E.; Eremeev, S. V.; Postnikov, A. V.; Bazhanov, D. I.; Potapkin, B. V. *Semiconductors* **2007**, *41*, 810.
(22) Galitsyn, Yu. G.; Dmitriev, D. V.; Mansurov, V. G.; Moshchenko, S. P.; Toropov, A. I. *JETP Lett.* **2005**, *81*, 625.